Contractor Report ARWEC-CR-98015

MICROSTRUCTURE AND MIXING DISTRIBUTION ANALYSIS IN M30 TRIPLE-BASE PROPELLANTS

Rahmi Yazici
Dilhan M. Kalyon
Stevens Institute of Technology
Castle Point on Hudson
Hoboken, NJ 07030

David Fair
Project Engineer
ARDEC

September 1998

US ARMY
TANK AUTOMOTIVE AND
ARMAMENTS COMMAND
ARMAMENT RDE CENTER

U.S. ARMY ARMAMENT RESEARCH, DEVELOPMENT AND ENGINEERING CENTER

Warheads, Energetics & Combat-support Armaments Center

Picatinny Arsenal, New Jersey

The views, opinions, and/or findings contained in this report are those of the author(s) and should not be construed as an official Department of the Army position, policy, or decision, unless so designated by other documentation.

The citation in this report of the names of commercial firms or commercially available products or services does not constitute official endorsement by or approval of the U.S. Government.

Destroy this report when no longer needed by any method that will prevent disclosure of its contents or reconstruction of the document. Do not return to the originator.

REPORT DOCUMENTATION PAGE

Form Approved
OMB No. 0704-0188

1. AGENCY USE ONLY (Leave Blank)	2. REPORT DATE	3. REPORT TYPE AND DATES COVERED
	September 1998	Interim/Mar 96 to Feb 97

4. TITLE AND SUBTITLE
MICROSTRUCTURE AND MIXING DISTRIBUTION ANALYSIS IN M30 TRIPLE-BASE PROPELLANTS

5. FUNDING NUMBERS

6. AUTHOR(S)
Rahmi Yazici and Dilhan M. Kalyon, Stevens Institute of Technology
David Fair, Project Engineer, ARDEC

7. PERFORMING ORGANIZATION NAME(S) AND ADDRESS(ES)

Highly Filled Materials Institute
Stevens Institute of Technology
Castle Point on Hudson
Hoboken, NJ 07030

ARDEC, WECAC
System Readiness Center
(AMSTA-AR-WES)
Picatinny Arsenal, NJ 07806

8. PERFORMING ORGANIZATION REPORT NUMBER

9. SPONSORING/MONITORING AGENCY NAME(S) AND ADDRESS(ES)

ARDEC, WECAC
Information Research Center (AMSTA-AR-WEL-T)
Picatinny Arsenal, NJ 07806-5000

10. SPONSORING/MONITORING AGENCY REPORT NUMBER

Contractor Report
ARWEC-CR-98015

11. SUPPLEMENTARY NOTES
This project was accomplished as part of the U.S. Army's ARDEC Advanced System Integration Division program. The primary objective of this program is to develop, on a timely basis, manufacturing processes, techniques, and equipment for use in production of Army material.

12a. DISTRIBUTION/AVAILABILITY STATEMENT

Approved for public release; distribution is unlimited.

12b. DISTRIBUTION CODE

13. ABSTRACT

Two different lots of M30 triple-base propellants, RAD-MEI-049 and RAD-MEI-051 (lots 49 and 51), were analyzed to determine the degree of mixing and distribution of the components in the propellant grains using novel x-ray diffraction techniques developed at Stevens. The degree of mixing was relatively low in both lots; with lot 49 being better than lot 51. The mixing index of nitroglycerine (NG) was inferior in both lots when compared to nitrocellulose (NC) and nitro-guanidine (NQ). The mixing distribution analysis of the components in the propellant grains showed enrichment of NQ and NC, and depletion of NG at the center. The reverse was true at the surface of the grains. Depletion of NQ in the grain interior and migration to the grain surface was evident in both lots. It was conclued that some of the NG is un-bound and acts as a lower viscosity fluid during extrusion and migrates to the surface. Other processing defects observed in the M30 grains were formation of voids and internal cracks, and presence of wavy perforations. (cont)

14. SUBJECT TERMS
Triple-base Propellants Degree-of-mixing NQ NG NC
Mixing distribution X-ray diffraction

15. NUMBER OF PAGES
37

16. PRICE CODE

17. SECURITY CLASSIFICATION OF REPORT	18. SECURITY CLASSIFICATION OF THIS PAGE	19. SECURITY CLASSIFICATION OF ABSTRACT	20. LIMITATION OF ABSTRACT
UNCLASSIFIED	UNCLASSIFIED	UNCLASSIFIED	SAR

13. ABSTRACT (cont)

The alignment of the NQ particles along the extrusion axis of the grains was high in both of the lots; however, it suffered at the near-surface regions. The average particle diameter of NQ whiskers was larger in lot 49 than in lot 51.

Future work is recommended for comprehensive and systematic evaluation of the mixing distribution and microstructure of the M30 triple-base propellants as affected by controlled processing parameters. Such systematic work in collaboration with ARDEC should offer significant cost saving insights for the process and production, and opportunities for improved quality of M30 triple-base propellants.

ACKNOWLEDGMENTS

This research was supported by the contract #N00014-95-1-1258 by US Army Armament Research, Development and Engineering Center and managed by Olin Ordnance Corp. The program directors were David Fair and Richard S. Miller. We are grateful for this support. The propellants were provided by Olin Ordnance Corp. and the calibration samples were provided by William Ansley of NSWC/IH Division. We are thankful for their contributions.

CONTENTS

FIGURES

TABLES

SUMMARY

In this investigation, two different lots of M30 triple-base propellants, RAD-MEI-049 and RAD-MEI-051 (lot 49 and 51), were analyzed to determine the degree of mixing of the components and the distribution of the mixedness in the propellant grains using novel x-ray diffraction (XRD) techniques developed at Stevens. The microstructural features including the nitroguanidine (NQ) particle size and orientation, and the processing defects were evaluated.

The results of this work revealed an NQ degree of mixing index (MI) of 0.90 and 0.88 for the lot 49 and 51 grains, respectively, at 1.2 mm^2 scale of examination. The degree of mixing in lot 49 was slightly better than in lot 51. The distribution of mixedness of the components in the propellant grains showed enrichment of NQ and nitrocellulose (NC), and depletion of nitroglycerine (NG) at the center. The reverse was true at the surface of the grains. The mixing-index (MI = 0.72) of NG was inferior when compared to NC (MI = 0.82) and NQ (MI = 0.88). The mixing distribution analysis showed depletion of NG in the interior of the grains and NG migration to the surface regions, in both lots. These results, obtained by the novel XRD method, indicated that a substantial portion of NG and the residual solvents are not effectively bound to the NC matrix and act as an immiscible, lower-viscosity fluid during extrusion and migrates to the surface regions of the propellant grains.

The principal processing defects observed in the M30 grains were voids and cracks along the longitudinal axis, and presence of irregular (wavery) perforations. Wavery features were prominent in lot 51, indicating a history of less suitable processing conditions. The average particle diameter of NQ whiskers was larger in lot 49 (5 μm) than in lot 51 (2.5 μm). The alignment of the NQ particles (whiskers) along the extrusion axis of the grains was high (0.95) in both of the lots; however, the degree of alignment has suffered at the near-surface regions.

Future work is recommended for comprehensive and systematic evaluation of the mixing distribution and microstructure of the M30 triple-base propellants as affected by controlled processing parameters. Such systematic work in collaboration with the U.S. Army Armament Research, Development and Engineering Center (ARDEC), Picatinny Arsenal, New Jersey should offer significant cost saving insights for the process and production, and opportunities for improved quality of M30 triple-base propellants.

INTRODUCTION

The energetic ingredients that go into solid propellants have to be metered accurately and mixed rigorously in order to secure a uniform microstructure and a uniform energetic behavior throughout the solid propellant. Inadequate mixing of the ingredients and formation of defects lead to production of inhomogeneous propellants with localized "sensitive" regions that seriously undermine the accuracy and the consistency of the energetic performance.

The techniques applied to characterize the degree of the mixedness of a composite such as a propellant would involve either direct or indirect methods. Indirect methods include the determination of some representative property including transmissive, reflective, resistivity, ultrasound, and

rheological properties. Such techniques are suitable for product quality control, where the relationship between the measured property and the ultimate property of interest is apriori known. However, although such techniques are useful, they are post-mortem and provide no direct quantitative data on how well the ingredients are interspersed in each other.

Some techniques involving incorporation of color tracers are also available for study of degree of mixedness (refs. 1 through 6). For example, Kalyon and co-workers (refs. 7 and 8) have employed color incorporated thermoplastic elastomers, followed by computerized image analysis, to investigate the distributive mixing of thermoplastic elastomers in the regular flighted and kneading disc elements of twin-screw extruders. Although all these techniques are useful for understanding and modeling of the mixing process under different processing modes, their applicability in the production environment of propellants is highly limited.

On the other hand, the rapid advent of imaging and sensing technology has facilitated the introduction of various powerful techniques, including the nuclear magnetic resonance (NMR) imaging and x-ray based techniques, to the analyses of opaque mixtures. Sinton and Yazici et al. (ref. 9) have employed magnetic resonance imaging, wide-angle XRD, and x-ray radioscopy to characterize the amount of air entrained into composite suspensions with elastomeric binders during extrusion processing, which is related principally to the degree of fill profile in the extruder. Yazici and Kalyon (refs. 10 and 11) have developed and applied electron probe and XRD techniques to the analysis of degree of mixing in solid-propellant simulants (ref. 10) and live LOVA propellants (ref. 11).

In this study, the analytical technique based on wide-angle XRD and developed by the authors to assess the degree of mixing in concentrated suspensions is applied to evaluate live M30 propellants. The applicability of this technique to the quantitative characterization of the distributive mixing achieved in two M30 triple-base propellant lots processed by batch mixing operations was demonstrated, comparatively. The investigation was carried out as an integral part of the processing design task of ARDEC.

PROGRAM GOALS

Apply analytical methods based on wide-angle XRD to:

- Identify various components in M30 triple-base formulations
- Quantitatively determine the volume fraction of each component and its distribution at various locations in the M30 triple-base propellant grains
- Quantitatively characterize the degree of mixing and mixing distribution of each component in the grains
- Develop a data base to assess the comparative state of mixedness of M30 triple-base propellant lots prepared by different mixing and processing modes

- Correlate processing/microstructure/performance relationships of energetic materials

EXPERIMENTAL PROCEDURES

Materials Selection

In this investigation, grain samples from two different lots of M30 triple-base propellants were chosen for analysis. The nominal M30 triple-base propellant formulation constitutes (by weight) 47.7% NQ, 28% NC, 22.5% NG, and 1.8% of other ingredients and additives. The formulation given in the MSDS of Hercules Inc., Radford, Virginia, is shown in table 1. Samples of the M30 extruded grains were acquired through ARDEC. The samples were chosen from two lots designated as RAD-MEI-049 and RAD-MEI-051 by ARDEC. These lots and will be called lot 49 and lot 51, respectively, in this report for simplicity.

Both of the M30 lots were processed by batch mixing of the triple-base formulation followed by ram extrusion. In addition to the main ingredients of the formulation listed in table 1, a mixture of methanol and acetone was used during batch mixing. The solvent content during mixing was approximately 22%. After a blow-down stage, the amount of residual solvents during extrusion were 11%. The mixed propellant is then blocked to consolidate it prior to extrusion. The 12-in. blocks are extruded in a vertical ram press. The extruded propellant is cut, dried in ovens, blended, and packaged for shipment.

The propellant grains are 0.5 in. in diameter and were received in transverse-sectioned forms of 0.05 in. in thickness and a limited number of 0.5 in. in thickness (fig. 1). The thin sections were not suitable for x-ray analysis because the beam fully penetrated the specimens generating background noise from the substrate. Longitudinal cross-sections were prepared from those relatively thick samples prior to characterization with XRD and electron microscopy (SEM) (fig. 2). Sectioning was carried-out with a guillotine. Some of the cross-sectional specimens for electron microscopy were prepared by fracturing. All sample preparation and handling was carried out according to the safety procedures outlined by ONR's safety officer, Robert Zaleski, who inspects Stevens facilities twice a year.

Characterization of the Mixing Indices

Various mixing indices were derived based on the statistical parameters of the experimental measurements and used to quantitatively characterize the degree of mixing of the two M30 propellant lots. Wide-angle XRD was used as the principal analytical method.

The relative volume-fractions of the solid ingredients and the binder were used as a measure of the degree of mixing of the samples, i.e., for NQ relative volume fraction NQ over the other ingredients (NC and NG) is given by

$$\text{NQ relative volume fraction} = \frac{\phi_{NQ}}{\left(\phi_{NC} + \phi_{NG}\right)} \tag{1}$$

In general, the quantitative description of the mixing quality or goodness of mixing of a given mixture can be developed by comparison of the state of the mixture to the most complete mixing state attainable (ref. 12). This complete mixing corresponds to statistical randomness of the ultimate properties of the ingredients being mixed which would follow the Binomial distribution (ref. 13).

If one makes N measurements of concentration, c_i of one of the components, then the mean concentration may be calculated according to

$$\bar{c} = \frac{1}{N}\sum_{i=1}^{N} c_i \tag{2}$$

where $\bar{c}$ should not differ significantly from the overall concentration of the component, ϕ unless a faulty sampling technique is used. The difference between $\bar{c}$ and ϕ decreases as the number of the characterized samples N is increased. The measured concentration values of the minor component also depend on the sample size. These values approach the overall concentration of the minor component ϕ as the sample size is increased.

A basic measure of the homogeneity of a mixture is the extent to which the concentration values at various regions of the volume of the mixture differ from the mean concentration. The variance s^2, arising from the individual concentration c_i measurements, provides such an index to quantitatively assess the degree of mixedness. The variance is given by

$$s^2 = \frac{1}{(N-1)}\sum_{i=1}^{N}\left(c_i - \bar{c}\right)^2 \tag{3}$$

A small variance implies that most of the samples yield concentration c_i values which are close to the mean $\bar{c}$ of all samples, thus suggesting a homogeneous system. The deviation of the sample measurements from the mean $\bar{c}$ is given by standard deviation

$$s = \sqrt{s^2} \tag{4}$$

which is defined as the square root of the variance, and is in the same units as the concentration data. When the means of two concentration data sets differ greatly, a measure of relative variability is defined with coefficient of variation, v, which is the ratio of standard deviation to mean (ref. 14)

$$v = \frac{s}{\bar{c}} \tag{5}$$

The maximum variance occurs if the components are completely segregated. Maximum variance is given by

$$s_0^2 = \bar{c}(1-\bar{c}) \tag{6}$$

If the variance is normalized to its maximum value, the resulting parameter is called the intensity of segregation, I_{seg} (refs. 11 and 12). This is given by

$$I_{seg} = \frac{s^2}{s_0^2} = \frac{s^2}{\bar{c}(1-\bar{c})} \tag{7}$$

One can then define the intensity of mixing as

$$I_{mix} = 1 - \frac{s^2}{s_0^2} \tag{8}$$

A distributive mixing index, MI, can be defined as

$$MI = 1 - \frac{s}{s_0} \tag{9}$$

Both the intensity of mixing and the MI values approach to one for ideally homogeneous systems.

In this study, it was found that coefficient of variation (v), intensity of mixing (I_{mix}), and mixing index (MI) are all additional important indices in evaluating degree and distribution of mixing. The mixing indices and the statistical parameters used in this work are summarized in table 2.

Analytical Technique: Wide-Angle X-Ray Diffractometry

X-ray diffractometry has been successfully applied for both qualitative and quantitative phase analysis in multi-phase materials (refs. 15 and 16). Upon irradiation with x-rays, a given substance produces a characteristic diffraction pattern. Diffraction is essentially a scattering phenomenon in which a large number of atoms (or molecules) in the crystalline material, arranged periodically on a lattice, scatter the x-rays in phase. These phase relations are such that destructive interference occurs in most directions of scattering, but in a few directions constructive interference takes place and diffracted beams are formed. According to Bragg Law, the diffracted beams make a 2θ angle with respect to the incident beam, i.e.,

$$\lambda = 2d\sin\theta \tag{11}$$

where λ is the wavelength of the x-rays of the incident beam and d is the spacing between the atomic (lattice) planes of the crystalline material which make a θ angle with respect to the incident

beam. Because the d-spacings between atomic planes and their distribution in space (the crystal structure) is unique for each material, the angular distribution of the diffraction peaks and their intensities (the diffraction pattern) is also unique for a particular material. Qualitative analysis by XRD is accomplished by identification of the particular diffraction pattern of a substance from the standard diffraction data bases (ref. 17). In the amorphous materials, on the other hand, the atoms (and molecules) exhibit short-range order, in clusters of a few atomic (or molecular) distances, and lack long-range order. Such amorphous structures give rise to very broad x-ray scattering peak(s) centered around the corresponding characteristic interatomic (and intermolecular) distance(s). Identification of an amorphous material using the broad x-ray scattering pattern can be achieved by carrying out control x-ray scattering experiments with standard samples of the same material.

The particular advantage of XRD analysis is that it discloses the presence of a substance, as that substance actually exists in the sample, and not in terms of its constituent chemical elements. If the sample contains more than one compound or phase that constitute the same chemical elements (or element groups), all these compounds are disclosed by diffraction analysis. Quantitative analysis is also possible because the intensity of the diffraction pattern of a particular phase - in a mixture of phases - depends on the concentration of that phase in the mixture. The relation between the integrated intensity I_i and the volume fraction ϕ_i of a phase is generally nonlinear since diffracted intensity depends strongly on the absorption coefficient of the mixture, μ_m, which itself depends on the concentration. For a two-phase material (with absorption coefficients μ_1 and μ_2 for the in-dividual phases), the absorption coefficient for the mixture becomes

$$\mu_m = \phi_1 \mu_1 + \phi_2 \mu_2 \tag{12}$$

The integrated intensity from phase 1 is then given by (ref. 16)

$$I_1 = \frac{K_1 \phi_1}{\mu_m} \tag{13}$$

where K_1 is a constant that depends on the material and the incident beam used, but not on the concentration. The relative ratio of intensities from phases 1 and 2, however, is independent of μ_m and varies with concentration

$$\frac{I_1}{I_2} = \frac{K_1 \phi_1}{K_2 \phi_2} \tag{14}$$

where the K values can be determined either from the $I_i/I_{corundum}$ values listed by JCPDS (ref. 17) or by preparing standard samples of known composition.

As listed in table 3, the ingredients of the M30 triple-base propellants under study constitute of similar elements C-H-N-O and similar molecules, making it difficult to differentiate the ingredients in the propellant by the conventional analytical methods. Degree of mixing analysis, however, require positive identification and differentiation of each ingredient in a given mixture.

On the other hand, as listed in table 4, the ingredients of this formulation exhibit distinct crystallinity characteristics: NQ exhibits a unique crystal structure and NC + NG exhibit unique amorphous structures. Our wide-angle XRD technique then is a very effective method to differentiate and quantify the amounts of these ingredients present.

In this study, the relative volume fractions of NQ and NC + NG were calculated from the relative intensity fraction values which are unique to each ingredient. These measurements were carried out using a relatively high number of crystal-plane reflections of the crystalline NQ in order to eliminate texture effects and to increase accuracy (fig. 3). For amorphous NC + NG, the entire broad amorphous peak (fig. 3) was used.

The amorphous diffraction pattern of NC + NG was further deconvoluted to separate the contributions of the individual ingredients NC and NG. As shown in figure 4, deconvolution of NG from NC was achieved by taking advantage of the unique shape of the diffraction pattern of NC. The amorphous peak of NG is positioned at the same 2θ angle (22 deg) as the NC amorphous peak and makes it impossible to apply conventional deconvolution peak intensity evaluation techniques. However, during this investigation, a special method was developed based on the finding that as the amorphous diffraction pattern of NC exhibits a maxima, a "head", at around 22 deg 2θ it also exhibits a unique "shoulder" at the higher 2θ angles that extend up to 50 deg. The ratio of the diffracted intensity values at the head (~ 22 deg) and at the shoulder (~40 deg) positions of the NC pattern is constant for a given NC lot (refs. 19 and 20). In this investigation, the shoulder intensity value was used to deconvolute NC signal from NG signal as shown in figure 4.

A Rigaku DXR-3000 and a Siemens D-5000 computerized wide-angle diffractometer system were used in this investigation. In both systems, crystal monochromatized Cu K_α radiation at 40 KV and 20 mA was applied. Used in all runs were 0.15 and 0.6 deg receiving slits. The x-ray probe size was varied by using 1 deg to 0.1 deg primary beam slits. The effective x-ray probe size used in degree of mixing and mixing distribution analysis was 1.2 mm^2. The effective depth of penetration of the x-rays used in this technique was more than 0.5 mm. The depth of penetration was calculated according to (ref. 15)

$$x = \frac{K_x \sin\theta}{2\mu} \tag{15}$$

where μ is the linear absorption coefficient (8.4 cm^{-1}), θ is the beam angle, and K_x = 6.91 for >99% of information. The experimental parameters of the x-ray diffraction experiments are summarized in table 5.

RESULTS AND DISCUSSIONS

Degree of Mixing

A typical wide-angle XRD pattern of the M30 propellant at the transverse cross-section of the grains which constitute ~ 47.7% by weight NQ and 50.5% by weight NC + NG as obtained with Cu K_α radiation, is shown in figure 3a.

This is a convoluted pattern which includes diffraction peaks from all the ingredients present in the formulation. The ingredients present and the nature of their polyforms was first determined from these experimental diffraction patterns. Computer search/match and identification/elimination methods were applied using the documented crystallographic information listed in the JCPDS data bases (ref 16). It was concluded that the propellants constituted crystalline NQ and NC + NG in the amorphous forms. The crystallographic information is summarized in table 3. The deconvoluted diffraction signal of crystalline NQ is shown in figure 3b. In figure 3c, the deconvoluted but cumulative diffraction pattern of NC + NG amorphous ingredients is shown to demonstrate the phase identification process.

Quantitative information on the volume fraction of the ingredients present was obtained from the XRD patterns by integrating the relevant peaks of the ingredients. A reference sample of NC + NG (AA-6 double-base propellant) and a stabilized NG solution were used to calibrate the measurements. Other raw ingredients NC and NQ used in M30 propellants were not available for this investigation. Various computational methods were developed and used for quantitative studies. The contributions from the additives and the effects of the micro voids and strand perforations were omitted from these calculations. The results of the quantitative XRD analysis of relative volume fractions of NQ and NC + NG are shown in tables 6 and 7, for 1.2 mm^2 scale of examination. The data from lot 49 and lot 51 are juxtaposed for comparison. The separated results of the relative volume fractions of NC and NG are shown in tables 8 and 9, respectively.

The statistical parameters obtained from the degree of mixing analysis at 1.2 mm^2 scale of examination indicated that the mixing index of the two M30 lots were relatively low when compared to other particulate propellants (ref. 11). The mixing indices of NC (MI = 0.82) and NG (MI = 0.72) were considerably low. Especially the value MI = 0.72 of NG in both propellant lots indicated an inherent processing problem that needs to be addressed with further studies. These results also showed small but detectable differences between the two lots, lot 49 and lot 51. The coefficient of variation (CV) parameter was most sensitive to reveal the subtle differences in mixing quality between the two lots. As listed in tables 6 through 9, the CV values for lot 49 are consistently lower than those of lot 51, indicating better degree of mixing in lot 49 than lot 51. Poor distribution of NG in both lots and the availability of limited samples with adequate thickness have both contributed to the small statistical differences observed between the two lots.

Mixing Distribution

The most striking results were observed in the distribution of mixing analysis. As shown in figures 6 and 7, in both lots the middle of the grains were depleted in NG and enriched in NC and NQ. According to these results, NG content decreased to a 10% level or below in the center of the propellant grains and increased to 25% level or above near the surface of the grains. Similar NG variation trends were also observed in the AA-6 double-base 4-in. diameter propellant grains and 5-mm diameter extrudates that were analyzed earlier at Stevens (ref. 19).

The migration of NG to grain surfaces from the interior could take place due to the thermo-mechanical history applied during extrusion of the propellants. In a previous investigation by Baker et al. (ref. 20), dielectric studies showed that in NC + NG mixtures when the concentration of NG is above 27%, the interaction between the adsorbate (NG) and the adsorbent (NC) is considerably

weakened. This weakening point approximately corresponds to the monolayer coverage of NC fibrular structure by NG (refs. 20 and 21). Addition of NG in excess of 27% leads to multilayer adsorption type of behavior where the NG molecules are more free to move than those in the first adsorbed layer. Furthermore, it has been shown that the amount of NG that goes into the adsorbed layer varies as a function of the level of nitration of NC, that is, the 27% NG adsorption monolayer value is characteristic for NC with 12.2% nitration and if the NC nitration is increased to 13.4%, for example, the amount of the NG adsorption monolayer drops below 27% due to the decrease in adsorption sites on NC with higher nitration (ref. 22). The NG molecules in excess of the monolayer adsorption maintain a "liquid-like" environment (ref. 20). This means that NG in excess of 27% in a NC + NG mixture will act as an unbound liquid, and be prone to migration during processing such as extrusion. Also, the presence of a filler such as NQ or RDX was shown not to affect seriously the amount of "adsorbed" NG (27% of NC + NG) and the "liquid-like" free NG [excess of 27% of NC + NG (ref. 22)].

These previous studies (refs. 20 and 22) are in good agreement with the findings of this investigation. In the M30 triple-base propellants that are investigated in this study, the NG content of the NC + NG mixture (binder) is 45%, substantially higher than the anticipated monolayer requirement of 27% and the excess NG is anticipated to be prone to migration during extrusion. The presence of solvents could further aggravate NG migration by diluting NG in the adsorbed layer and making more NG available for migration, and by driving NG to the surface during the solvent devolatilization stage after extrusion. Solvents, up to 11% of the full formulation, were also present during extrusion of the M30 propellant grains. Therefore, the effective liquid-like content of the NC + NG binder is 55%, more than twice that is required for monolayer coverage, during extrusion flows.

The M30 propellant grains are extruded with an annular capillary die where the material flow with non-uniform shear rate $\dot{\gamma}(r)$ and velocity $V_z(r)$ distributions (Poiseuille flow) and where the shear rate is higher near the die walls (ref. 22). It is a well established fact that in such flow situations where a deformation rate distribution exists and where two immiscible polymeric fluids of different shear viscosity behavior are flowing, the separation of the two fluids is expected, whereby the less viscous ingredient migrates or "exudes" to the high shear rate region (towards the walls of the capillary die) and encapsulates the higher viscosity ingredient (refs. 23 and 24). This is probably the principal mechanism that causes the enrichment of NG near the extrudate surfaces. The excess NG (and the sol-vent) above the 27% monolayer formation level, act as the less viscous fluid that migrates towards the walls of the grains. The extent and nature of the NG migration would, therefore, depend on the extrusion processing conditions applied. That is, the higher the extrusion rates and pressures the more pronounced the NG migration would be. Indirect evidence of such effects were found with dielectric and thermal analytical techniques (refs. 20 and 22) that showed the relaxation of low frequency "alpha peak" to be a function of the extrusion rate. Furthermore, in double-base propellants, extrusion of the grains is followed by an "annealing" stage at higher temperatures (60° to 80°C). Annealing relaxes the residual stresses and the residual microstructure induced during extrusion. Upon annealing, the propellants attain more uniform ultimate properties indicating better distribution of NG (ref. 22). The effects of processing parameters such as extrusion rate and pressure and annealing on NG distribution in MK93 (AA-6) double-base propellants are also currently being investigated by our group (ref. 19).

Defect Microstructure

In addition to the XRD measurements, extensive work was carried out SEM in search of the structural features that are relevant to this investigation.

The most prominent defects observed in microscopic analysis were voids and cracks in the propellants, which are signs of poor mixing of the ingredients and poor wetting/bonding of the NQ particles by the binder. A typical longitudinal cross-section of lot 51 is shown in figure 7a where the void and crack defects are marked. Another type of defect observed in lot 51 was formation of irregular (wavy) perforations. As can be seen in figure 7a, the long cracks run parallel to the perforation curvature, pointing to the same process problem. Cracks and voids were also common in the lot 49 grains as shown in figure 7b.

Nitroguanidine Particle Size and Orientation

Nitroguanidine particle size measurements were carried out using SEM. Typical micrographs taken from transverse cross-sections are shown in figures 8a and 8b. In general, lot 51 exhibited finer NQ particles than lot 49. Particle diameter ranged from 1 mm to 4 mm in lot 51 with an average diameter of 2.5 mm. In lot 49, on the other hand, particle diameter ranged from 2 mm to 8 mm with an average diameter of 5 mm. The length of the particles were very difficult to determine with microscopy in the consolidated propellants. The particle length was typically between 20 mm and 120 mm with a very large error margin. According to the SEM analysis, in some of the propellant grains there was evidence of the presence of finer NQ grains at the surface layers (fig. 9). It is possible that the finer NQ particles are generated through particle attrition and accumulated at the surface regions during processing. We recommend the application of our novel XAPS technique to further investigate the particle size distribution in these propellants.

Particle orientation and its distribution was determined by XRD method. As shown in figures 10a and b, respectively, the diffraction patterns obtained from the longitudinal and transverse cross-sections of the grains with respect to the grain axis differ considerably. This is due to the alignment of the high-aspect-ratio NQ particles with the grain axis during extrusion. The crystal growth habit of NQ particles is such that the prismatic planes are stacked up parallel to the long axis of the particles giving rise to high intensities in prismatic (240) and (420) peaks in the longitudinal cross-section (fig. 10a), whereas in the transverse cross-section (fig. 10b), the inclined near-basal planes, (131) and (311) with respect to particle axis, exhibit high intensities.

In this investigation, such measurements were carried out quantitatively to evaluate the state of the alignment of the NQ particles in lot 49 and lot 51. In both lots, the average degree of alignment was better than 95%. Both lots exhibited local variations in their particle alignment. In general, the particle alignment was relatively lower at the near-surface regions ($> 0.8\ r/r_0$), compared to the other regions of the propellant grains.

These same regions were also shown to be rich in NG in the mixing distribution analysis. These are the regions where excess NG and solvents migrate and where sort of a "relaxation" of the particle alignment takes place. These less aligned regions also exhibit more void space (fig. 9).

Probably, a similar "relaxation" mechanism is operative near the free surface that was also observed in some of the wavy perforations. Particle alignment, or lack of it, and its relaxation can be used to gauge the process parameters such as binder distribution, wetting, extrusion history, and others. The x-ray technique we have applied in this investigation is very powerful in determining particle orientation because it quantitatively determines the particle orientation from the direct measurements of the number of crystal planes present with respect to the grain axis. We recommend, therefore, these particle alignment measurements to be a part of the future work on M30 propellants.

CONCLUSIONS

1. Our x-ray diffraction (XRD) technique has:

   - Identified all principal components present in propellant formulation, i.e., nitroguanidine (NQ), nitrocellulose (NC), and nitroglycerine (NG)
   - Quantitatively determined the weight fraction of each component
   - Quantitatively characterized the degree of mixing of each component at a desired scale of examination, 1.2 mm^2
   - Quantitatively determined the mixing distribution across the propellant grains

2. The quality of mixing as measured by mixing indices of the two M30 propellant lots, especially that of the NG component, were relatively low compared to other propellants filled with particles.

3. Nitroglycerine was depleted at the interior of the grains and was enriched at near surface regions.

4. The nature of the NG phase distribution and the distribution of the voids indicated the unbound liquid-like behavior of the "excess" NG and its migration to the surface together with the solvent during extrusion of the grains.

5. Nitroglycerine particle size was different for the two lots. The average NQ whisker diameter was 5 μm in lot 49 and was 2.5 μm in lot 51.

6. The NQ particle orientation distribution was determined quantitatively by XRD and showed high alignment with grain axis in both lots, except at near-surface regions

7. Relatively high void formation and internal cracks were observed in both M30 lots

FUTURE WORK

The following are recommended as future work to follow-up the findings of this invest-igation and to produce better extruded grains in M30 triple-base propellants:

- Systematic study of the effects of controlled processing parameters on mixing distribution, especially those of extrusion rate, pressure, and annealing
- Analysis of nitrocellulose (NC) with different cellulose sources and degree of nitration and to establish a reference base for evaluation of NC based propellants
- Analysis of the effect of processing on nitroguanidine particle size distribu-tion, orientation, and particle defect structure
- Analysis of more M30 lots, especially those which exhibit unique burning rate characteristics and correlation of the field performance of propellants with the mixing distribution, orientation, and defect structure

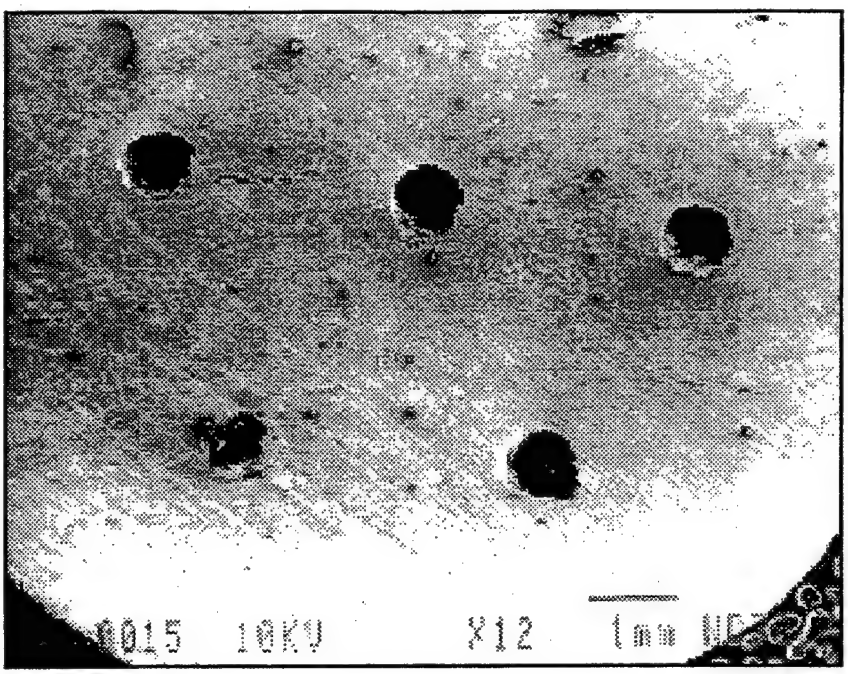

Fig.1. M-30 triple base propellant typical transverse cross section

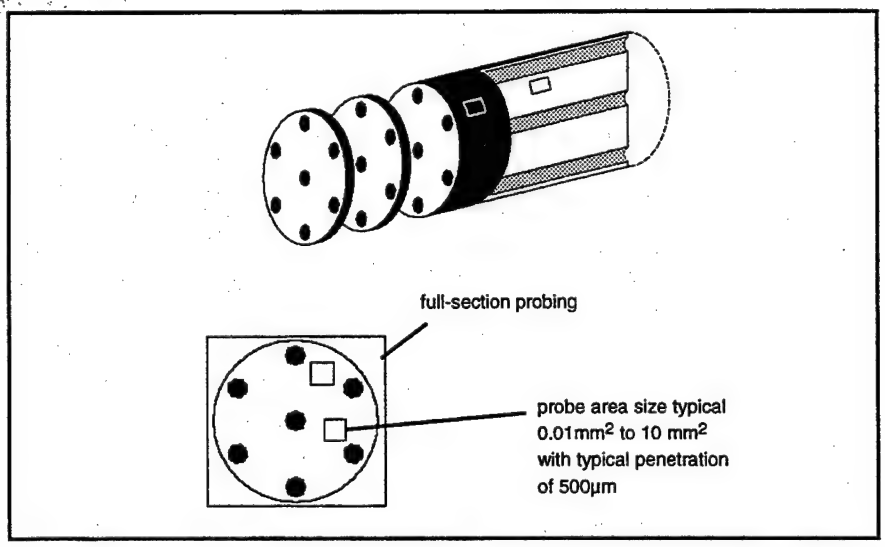

Fig.2. Sectioning of the extruded propellant grain in the transverse and longitudinal directions and probing with x-ray beam.

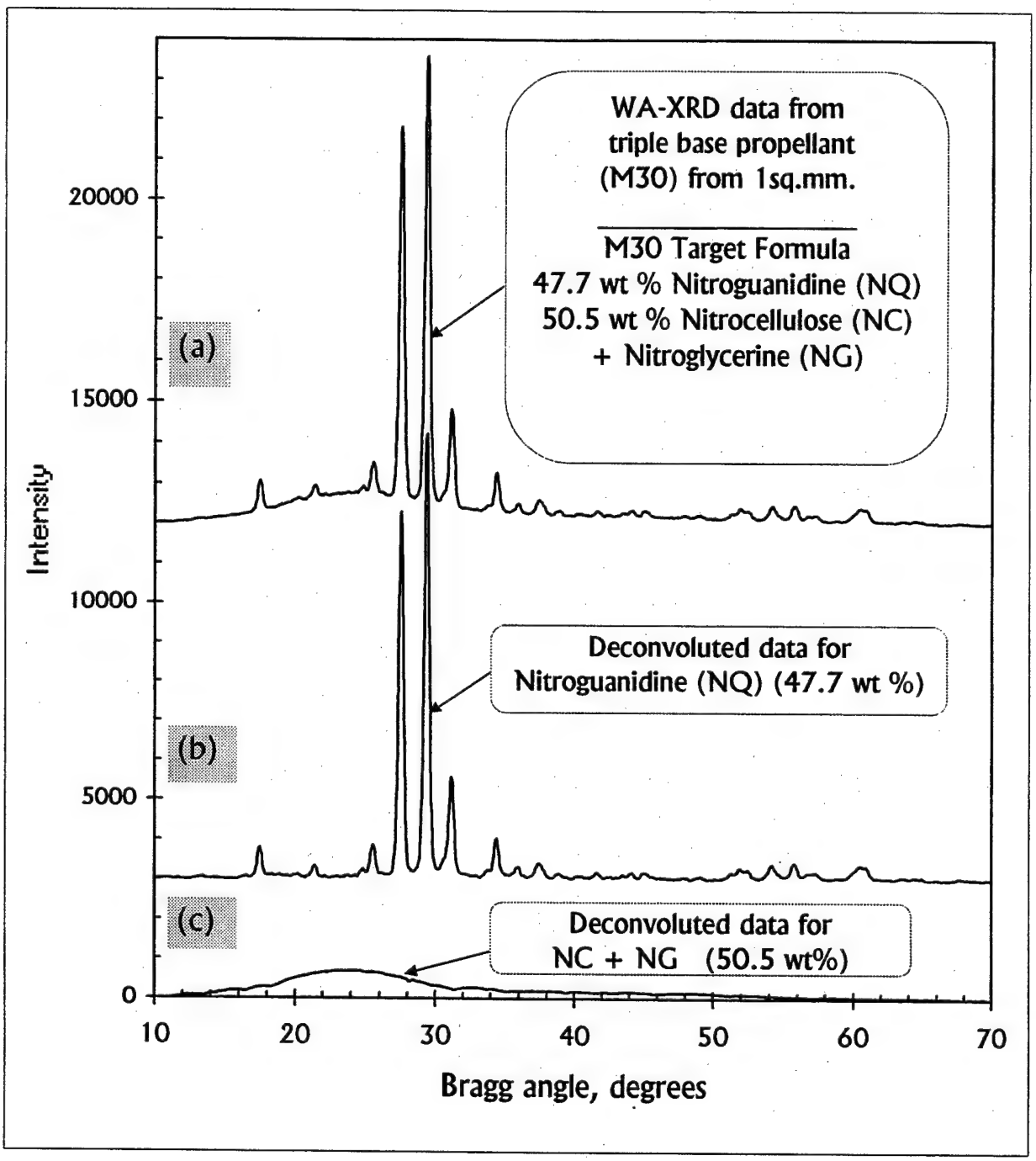

Fig. 3 Seperation of the NQ signal from NC + NG

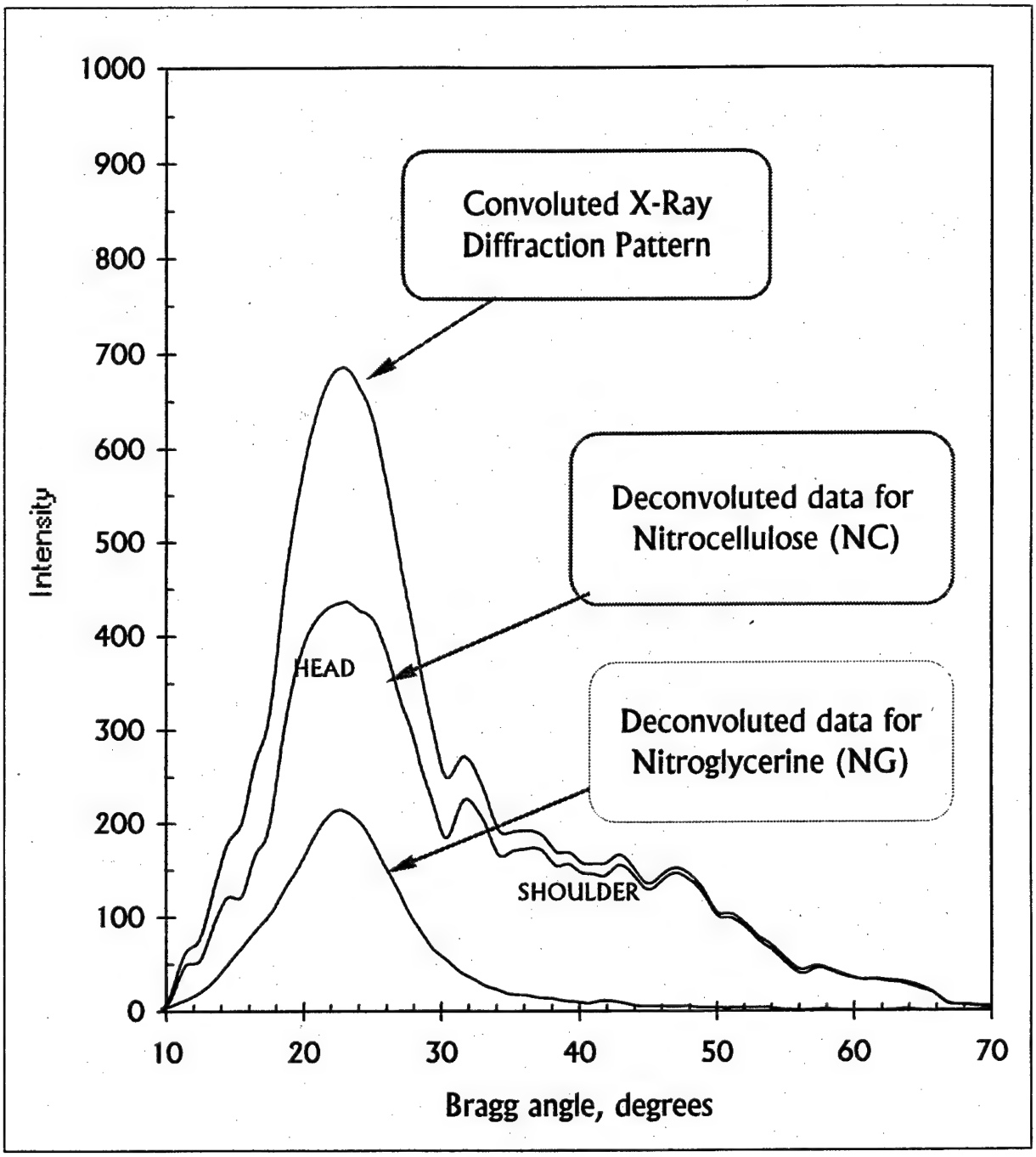

Fig. 4 Seperation of the NC and NG signals from the convoluted x-ray diffraction pattern

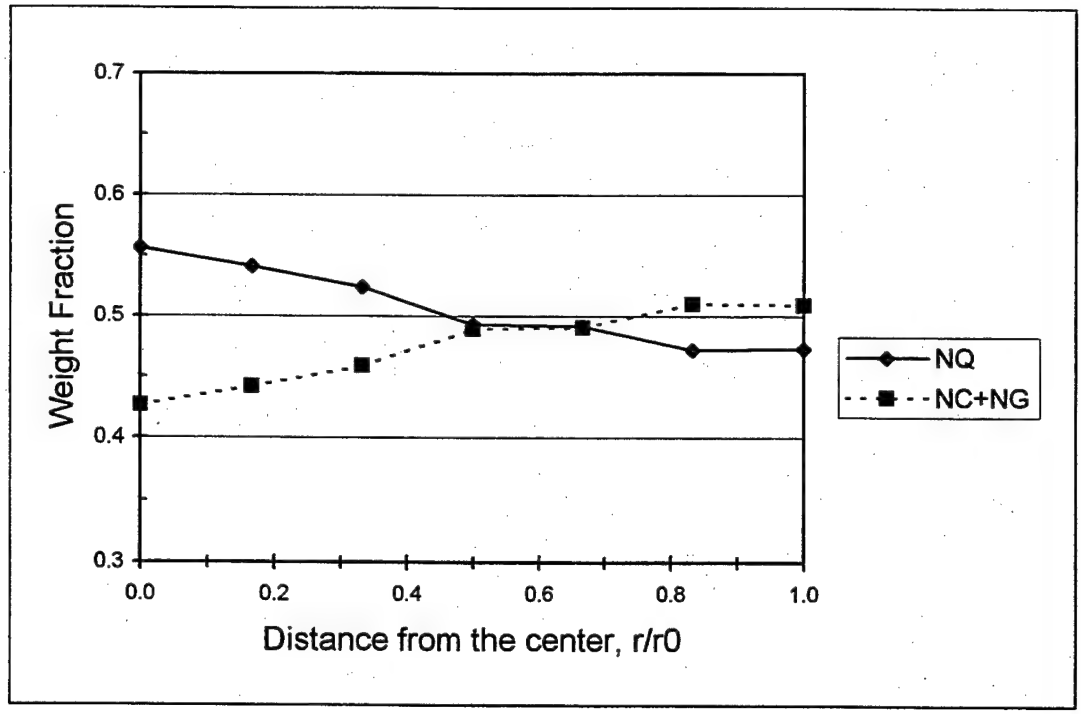

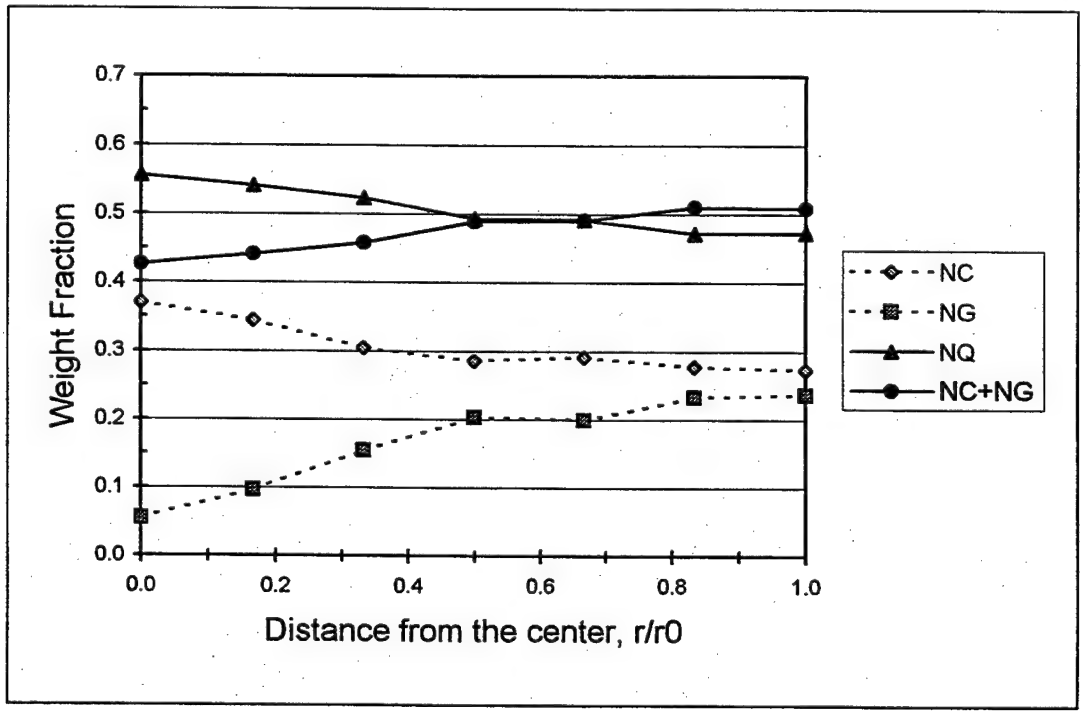

Fig. 5 Variation of components in the cross section of M30 Lot-49 triple- base propellant

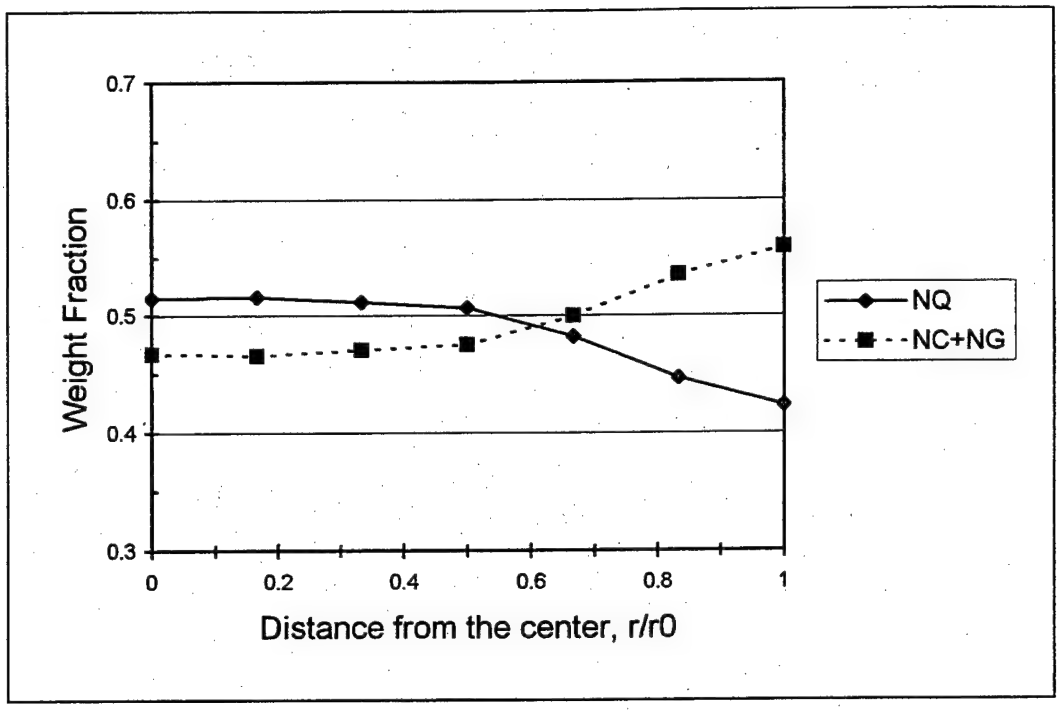

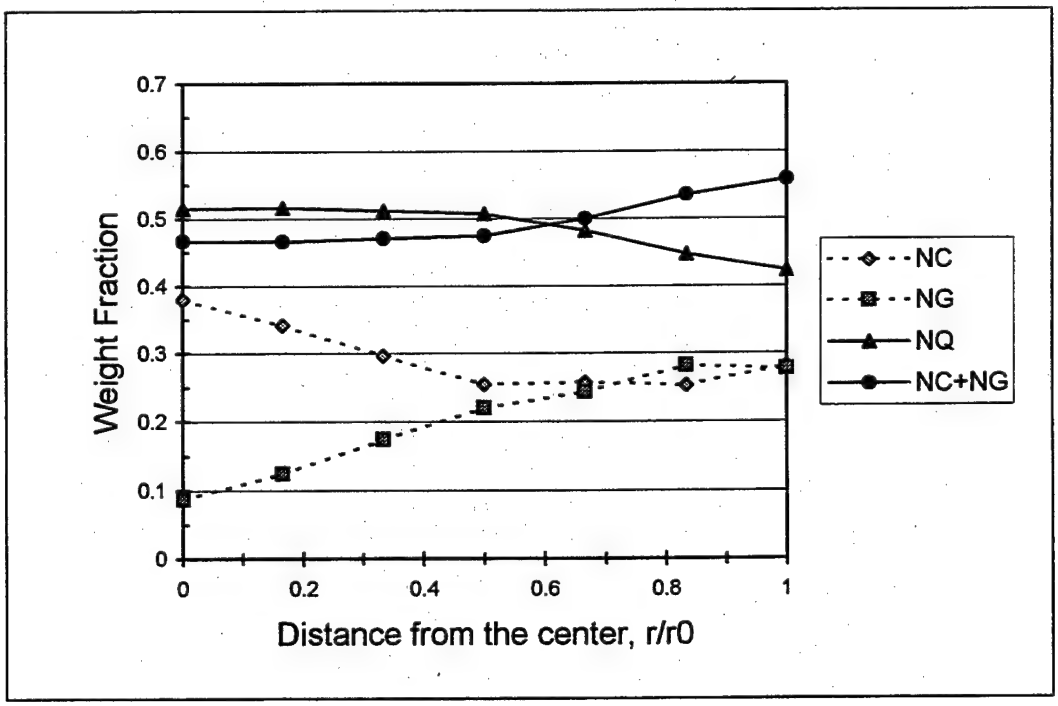

Fig. 6 Variation of components in the cross section of M30 Lot-51 triple- base propellant

a)

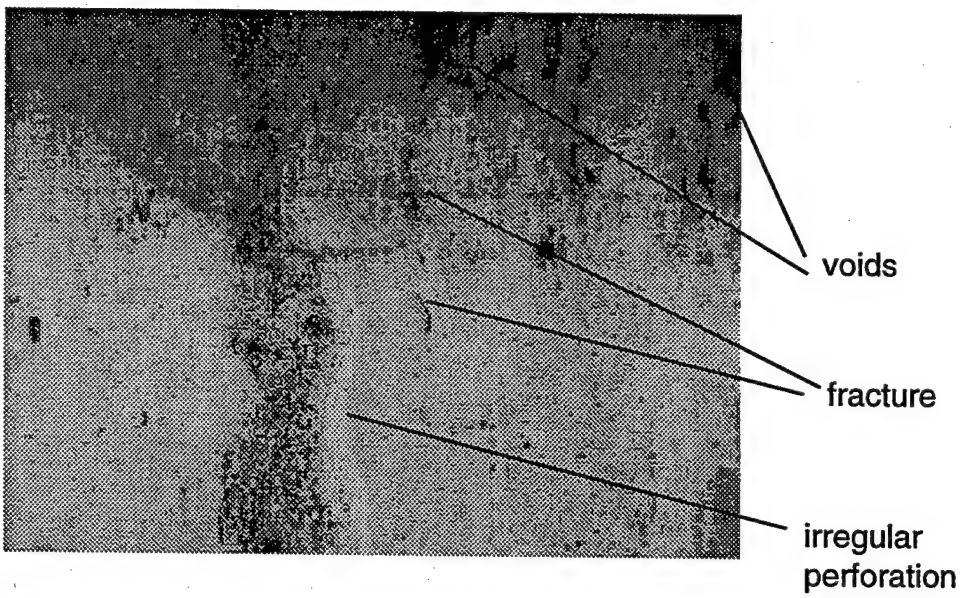

b)

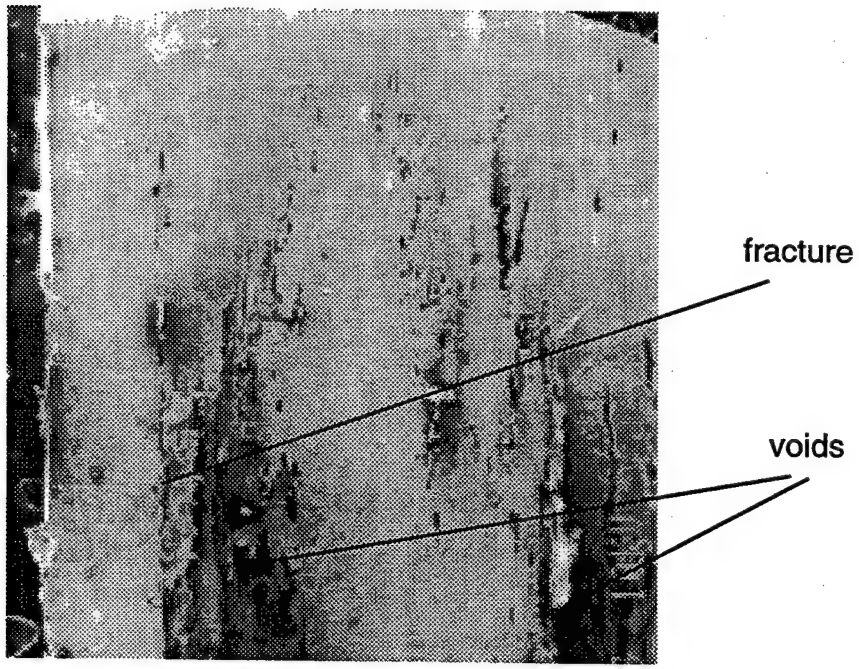

Fig.7. M-30 triple base propellants (15x):
(a) Lot 51 cut cross section showing processing defects: irregular (wavy) perforation, fracture formation parallel to the perforation, and void formation,
(b) Lot 49 cut cross section showing processing defects: void formation and fracture formation parallel to the grain axis.

a)

b)

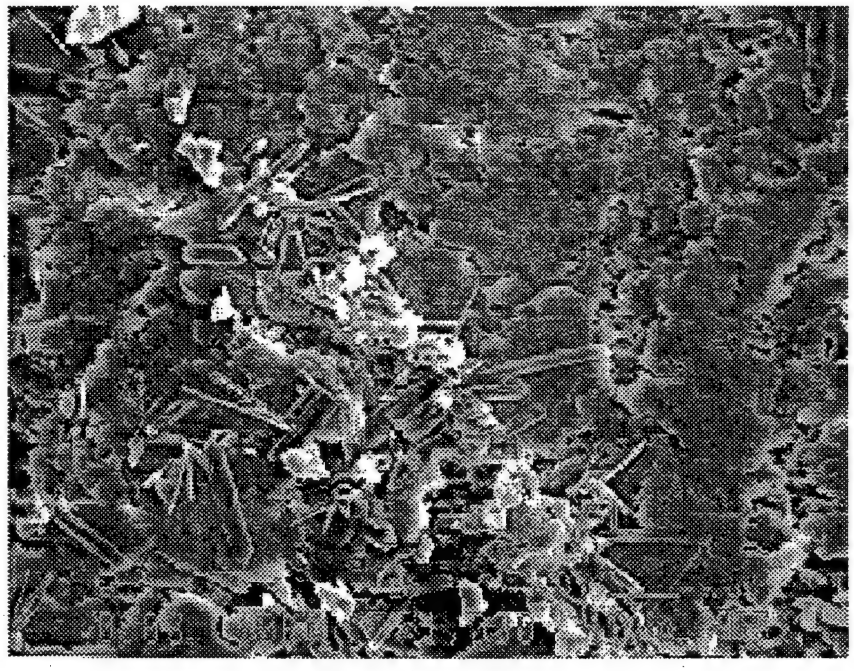

Fig. 8 Transverse cross sections of M-30 propellant grains (1000x) showing typical NQ whiskers in: (a) Lot 49, with 5 μm average whisker diameter, and (b) Lot 51, with 2.5 μm average whisker diameter.

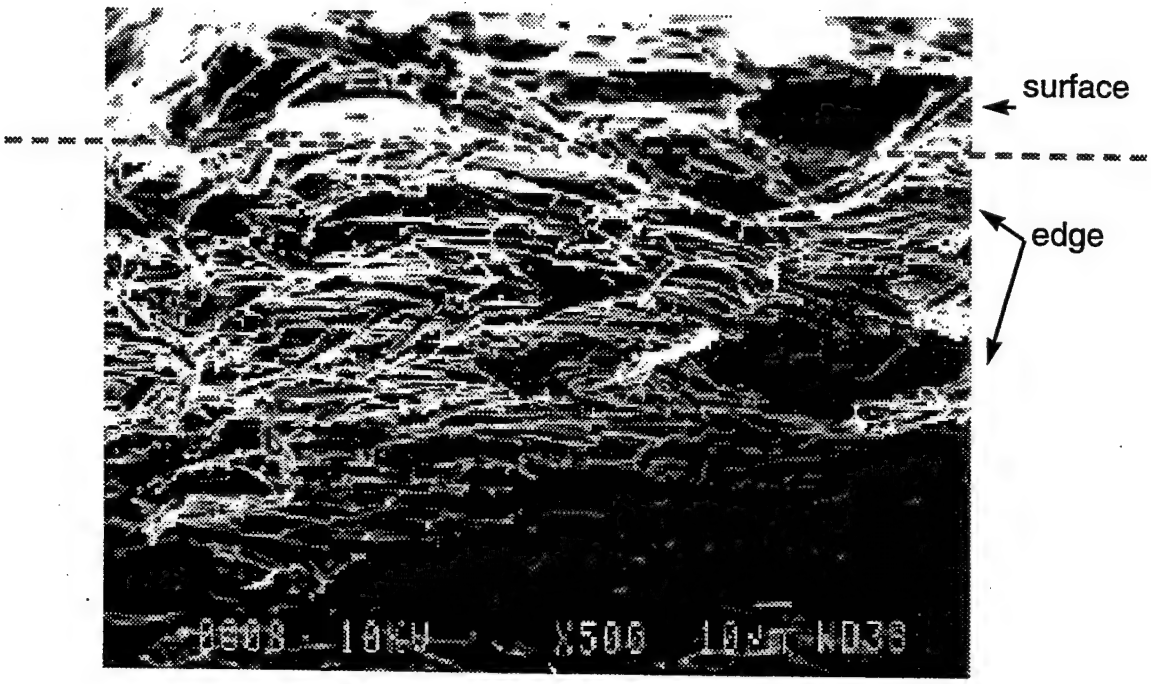

Fig. 9 Longitudinal cross section (500x) of a Lot 49 grain showing fine NQ particles at the edge near the surface with large interparticle spacing, lack of alignment and void formation.

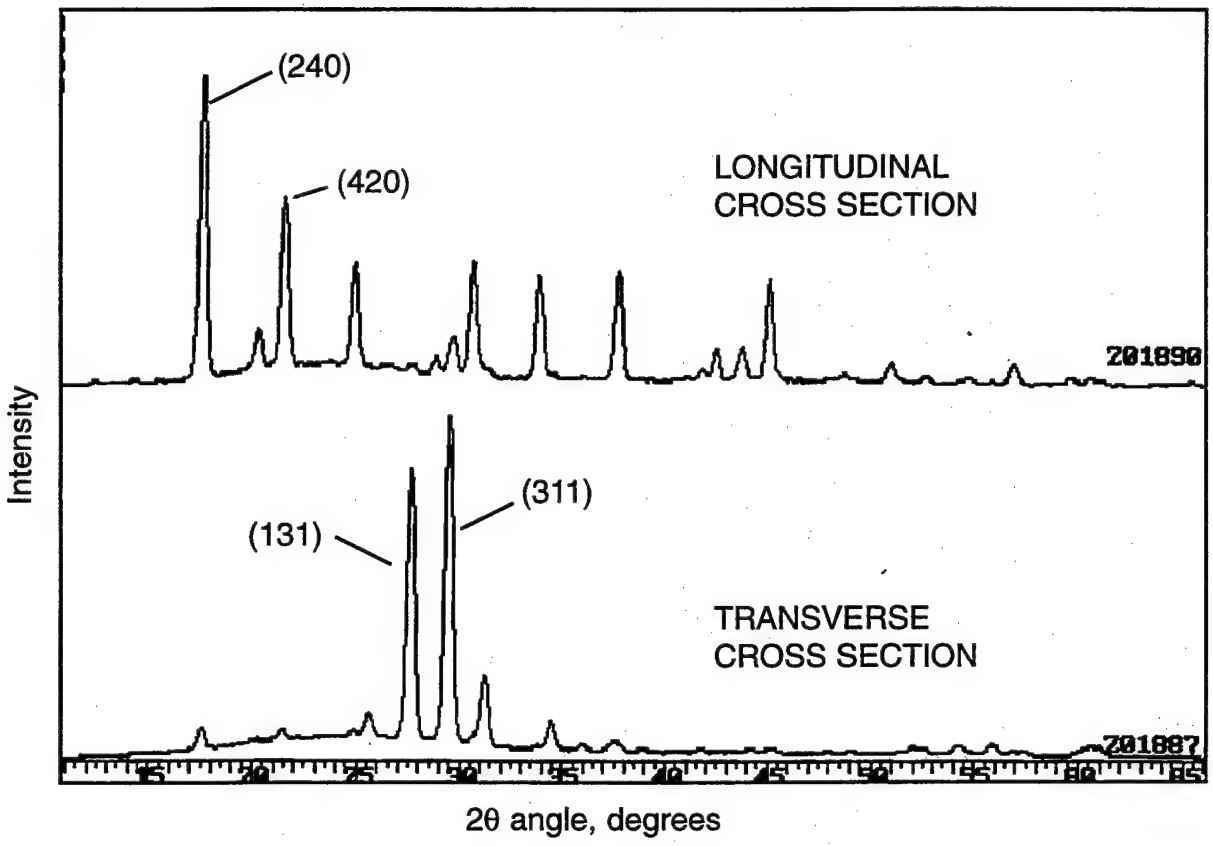

Fig. 10 WAXRD of M30 triple base propellant at (a) longitudinal cross section and (b) transverse cross section, showing the degree of alignment of the NQ particles. The variation of the high intensity peaks from the (240) and (420) prismatic planes, and (131) and (311) near-basal planes are used as a measure of the degree of NQ alignment along the grain axis.

Table 1. M30 formulation

Ingredient	Weight %	Density	Volume %
Nitroguanidine (NQ)	47.7	1.93	39.3
Nitrocellulose (NC)	28.0	1.23	36.2
Nitroglycerine (NG)	22.5	1.59	22.5
Ethyl-centralite	1.5	1.23	1.9
Cryolite	0.3	2.95	> .1
Total	100.0	1.588	100

Table 2. Mixing indices

mean: $$\bar{c} = \frac{1}{N} \sum_{i=1}^{N} c_i$$

variance: $$s^2 = \frac{1}{(N-1)} \sum_{i=1}^{N} (c_i - \bar{c})^2$$

standard deviation: $$s = \sqrt{s^2}$$

coefficient of variation: $$CV = \frac{s}{\bar{c}}$$

mixing index: $$MI = 1 - s / s_0$$

maximum variance: $$s_0^2 = \bar{c}(1-\bar{c})$$

intensity of mixing: $$I_{mix} = 1 - s^2 / s_0^2$$

intensity of segregation: $$I_{seg} = s^2 / s_0^2$$

segregation index: $$SI = s / s_0$$

Table 3. M30 ingredients

Label	Name	Formula
NQ	Nitroguanidine	$CH_4N_4O_2$
NC	Nitrocellulose	$C_1H_4N_4O_2$
NG	Nitroglycerine	$C_3H_5N_3O_9$
	Ethyl-Centralite (1,3-diethyl-1;3-diphenylurea)	$C_{17}H_{20}N_{20}$
	Cryolite	AlF_6Na_3

Table 4. Crystal structure characteristics of main M30 ingredients

Name / Crystal Structure / Lattice Constants / Space Group / Density

NQ Orthorhombic
a = 17.59, b= 24.81, c = 3.589 (SG:Fdd2)
d $\simeq$ 1.93

NC Amorphous or
d = 1.23
Monoclinic
a = 12.2, b = 10.28, c = 9.73 , b = 126.6

NG Amorphous
d = 1.59

Table 5. X-ray diffraction experimental parameters

Parameter	Value
KV	40
mA	20
monochromator	graphite crystal
diverging slit size	1 deg, .1 deg
soller slit size	1 deg
receiving slit size	.15 deg, .3 deg, .6 deg
probe size	1.2 mm^2, 10 mm^2
depth of penetration	0.5-1.4 mm

Table 6. NQ statistical parameters at 1.2 mm^2 scale in M30 propellants

Relative volume fraction parameters	Lot-49	Lot-51
mean	48	48
standard deviation	4.8	6.0
coefficient of variation	.10	.13
mixing index	.90	.88

Table 7. NC + NG statistical parameters at 1.2 mm^2 scale in M30 propellants

Relative volume fraction parameters	Lot-49	Lot-51
mean	51	51
standard deviation	4.8	6.0
coefficient of variation	.09	.12
mixing index	.90	.88

Table 8. NC statistical parameters at 1.2 mm^2 scale in M30 propellants

Relative volume fraction parameters	Lot-49	Lot-51
mean	28	28
standard deviation	7.5	8.1
coefficient of variation .27	.2 9	
mixing index	.84	.82

Table 9. NG statistical parameters at 1.2 $sq.mm^2$ scale in M30 propellants

Relative volume fraction parameters	Lot-49	Lot-51
mean	23	23
standard deviation	10.6	11.7
coefficient of variation	.46	.51
mixing index	.72	.72

REFERENCES

1. Ottino, J. M., The Kinematics of Mixing: Stretching, Chaos and Transport, Cambridge University Press, 1989.
2. Morikawa, A., Min, K., and White, J.L., Int. Polym. Process, 4, p 23, 1989.
3. Rwei, S.P., Manas-Zioczower, I., and Feke, D. F.,. Polym. Eng. Sci., 30, p 701, 1990.
4. David, B., and Tadmor, Z., Int. Polym. Process, 3, p 38, 1988.
5. Gokboro, M. N., "Mixing in Single Screw Extruders," Ph.D. Thesis, U. of Bradford, 1981.
6. Kubota, K., Brzoskowski, R., White, J. I., Weissert, F. C., Nakajima, N., and Min, K., Rubber Chem. Technol., 60, p 924, 1987.
7. Kalyon, D.M., Gotsis, A.D., Yilmazer, U., Gogos, C.G., Sangani, H., Aral, B., and Tsenoglou, C., Adv. Polym. Technol., 8, p 337, 1988.
8. Kalyon, D. M. and Sangani, H. N., Polym. Eng. Sci., 29, p 1018, 1989.
9. Kalyon, D. M., Yazici, R., Jacob, C., Aral, B., and Sinton, S.W., Polym. Eng. Sci., 31, p 386, 1991.
10. Yazici, R. and Kalyon, D. M., Rubber Chem. Technol., 66, p 527, 1993.
11. Yazici, R. and Kalyon, D., J. Energetic Materials, 14, p. 57, 1996.
12. Kalyon, D. M., in Encyclopedia of Fluid Mechanics, Houston, TX, Gulf Publishing, Vol. 7, Ch. 28, pp 887-926, 1988.
13. Mohr, W.D., Processing of Thermoplastic Materials, E. Bernhard, Ed., Kreiger Publishing Co., Malabar, 1959.
14. Dieter, G. E., Engineering Design, McGraw Hill, New York, NY, 1983.
15. Cullity, B.D., Elements of X-Ray Diffraction, Addison-Wesley Pub., Reading, MA, 1986.
16. Alexander, L.E., X-Ray Diffraction Methods in Polymer Science, Kreiger Publ. Co., Malabar, 1985.
17. International Center for Diffraction Data, JCPDS Files, Swathsmore, PA, 1994.
18. Internal Report, Alliant Tech. Systems, Inc., Radford Army Ammunition Plant, Radford, VA (Feb. 1996).
19. Yazici, R. and Kalyon, D., unpublished work done for NSWC/IH Div., 1996-97.

20. Baker, F. S., Jones, M., Lewis T. J., Privett, G., Crofton, D. J. and Pethrick, R. A., Polymer 25, 815-820 (1984).
21. Lotmensev, Y. M. and Schneerson, R. N., Trudy Khimicheskoi Telnolog, 1, 126 1974.
22. Baker, F. S., Jones, M. and Privett, G., Proceedings ADPA, 3rd Int. Gun Prop. Symp., USA 1985.
23. Kalyon, D. M., Khemis, M., Plastics and Rubber Proc. and App., 8 157-64,1987.
24. Akay, G., Rheol. Acta, 18, 256-67 1979.
25. Lee, B. and White, J., Trans. Soc. Rheol. 18 (3) 467-92, 1974.

DISTRIBUTION LIST

Commander
Armament Research, Development and Engineering Center
U.S. Army Tank-automotive and Armaments Command
ATTN: AMSTA-AR-WEL-T (2)
AMSTA-AR-GCL
AMSTA-AR-WES (20)
Picatinny Arsenal, NJ 07806-5000

Defense Technical Information Center (DTIC)
ATTN: Accessions Division (12)
8725 John J. Kingman Road, Ste 0944
Fort Belvoir, VA 22060-6218

Director
U.S. Army Materiel Systems Analysis Activity
ATTN: AMXSY-EI
392 Hopkins Road
Aberdeen Proving Ground, MD 21005-5071

Commander
Chemical/Biological Defense Agency
U.S. Army Armament, Munitions and Chemical Command
ATTN: AMSCB-CII, Library
Aberdeen Proving Ground, MD 21010-5423

Director
U.S. Army Edgewood Research, Development and Engineering Center
ATTN: SCBRD-RTB (Aerodynamics Technology Team)
Aberdeen Proving Ground, MD 21010-5423

Director
U.S. Army Research Laboratory
ATTN: AMSRL-OP-CI-B, Technical Library
Aberdeen Proving Ground, MD 21005-5066

Chief
Benet Weapons Laboratory, CCAC
Armament Research, Development and Engineering Center
U.S. Army Tank-automotive and Armaments Command
ATTN: AMSTA-AR-CCB-TL
Watervliet, NY 12189-5000

Director
U.S. Army TRADOC Analysis Command-WSMR
ATTN: ATRC-WSS-R
White Sands Missile Range, NM 88002

Commander
Naval Air Warfare Center Weapons Division
1 Administration Circle
ATTN: Code 473C1D, Carolyn Dettling (2)
China Lake, CA 93555-6001

GIDEP Operations Center
P.O. Box 8000
Corona, CA 91718-8000